Yb^{3+} and Tm^{3+} ions as sensitizers for the Ho^{3+} infrared emission in $Gd_3Ga_5O_{12}$ garnet and up-conversion energy losses

A. Brenier, L. C. Courrol, C. Pédrini, C. Madej, and G. Boulon
Laboratoire de Physico-Chimie des Matériaux Luminescents, Université Claude Bernard-Lyon I, Batiment 205, 43 Boulevard du 11 Novembre 1918, 69622 Villeurbanne Cedex, France
(Received 1 March 1993)

A study of the Ho^{3+} 2-μm laser emission in $Gd_3Ga_5O_{12}$ using Yb^{3+} and Tm^{3+} ions as sensitizers is presented. We show by quantum-yield measurements that up-conversion energy losses are weak in the triply doped crystal. Models that describe the excited-state dynamics for both up- and down-conversion processes are given.

I. INTRODUCTION

The eye-safe 2-μm laser emission is usually obtained from the $^5I_7 \rightarrow {}^5I_8$ transition of Ho^{3+} ions in fluoride or oxide hosts. Because the final level of the transition is thermally populated at room temperature it is necessary to sensitize the holmium fluorescence. Er^{3+}, Tm^{3+}, and Cr^{3+} ions have been extensively used.[1-4] In particular from our previous work[5] we know the efficiency of the Tm→Ho energy transfers in $Gd_3Ga_5O_{12}$ (GGG). The Ho sensitization of means of Yb^{3+} ions is attractive because it allows a laser diode pumping between 920 and 975 nm. We show in this paper that efficient energy transfers Yb→Tm and Yb→Ho occur in GGG leading to an enhancement of the Ho infrared fluorescence by comparison of the one from the Ho-monodoped GGG in which absorption in this range of wavelengths is weak.

The counterpart of the presence of sensitizers is that they can introduce some kind of energy losses. For example a source of losses is the Ho→Tm back transfer when the Tm concentration increases.[6] Another usual source of losses is the up-conversion processes. They have been recently identified in the Tm-Ho system[7,8] and have been often described in the Yb-Er system,[9-11] in the Yb-Tm system[12,13] or the Yb-Ho system.[13,14] We identify in this work some up-conversion mechanisms from the Yb and Ho or Tm infrared levels towards the Tm and Ho visible levels. We have measured their quantum yields and we give an analysis of the excited-state dynamics induced by very short-pulsed excitations.

II. EXPERIMENTAL METHODS

The studied crystals have been grown in our laboratory by the Czochralski method. The concentration $C(l)$ of one dopant in a sample cut at a distance l (along the axis of the crystal) from the origin $l=0$ of the crystal, and its coefficient of segregation k have been obtained by using the well-known relations

$$C(l)/C(0)=[1-g(l)]^{k-1},$$

$$C(0)=kC(\text{melt}),$$

where $g(l)$ is the crystallized fraction of the melt at point l. The ratio $C(l)/C(0)$ is deduced from the absorption spectra of the dopant. The coefficient of segregation k of the Yb, Tm, and Ho ions have been found to be about 1.2. The concentrations of the dopants in the studied samples are gathered in Table I.

The absorption spectra were recorded with a Cary 2300 spectrophotometer. The luminescence spectra in the visible range were obtained with a Jobin-Yvon HRS1 monochromator (1.2-nm resolution/mm slits), a Hamamatsu R1477 photomultiplier or a RCA 31034 cooled photomultiplier (GaAs photocathode) after exciting the samples with a Quantel dye laser (resolution 0.1 cm^{-1}) pumped with a frequency-doubled YAG:Nd Quantel laser. In the infrared range we used a Jobin-Yvon H250 monochromator (16-nm resolution/mm slits) equipped with a North Coast Ge ADC 403 HS nitrogen-cooled germanium cell. A Raman shifter hydrogen cell was used for the infrared excitations. The decay kinetics were recorded with a digital Lecroy 9400 oscilloscope or a SR430 multichannel analyser. The up-conversion quantum yields were measured with a homemade integrating cylindrical cavity, the inside of which being coated with white highly reflective Eastman Kodak paint, providing a lambertian diffusion of light. The energy of the laser beam (up to 3 mJ/pulse), focused on the sample with a 15-cm focal lens, has been measured with a Scientech 362 joulemeter.

TABLE I. Composition of $Gd_{3(1-x-y-z)}Yb_xTm_yHo_zGa_5O_{12}$ crystals.

x	y at. %	z	Yb	Tm 10^{20} ions/cm^3	Ho
5	0	0	7.0	O	O
0	5	0	0	7.9	0
5	5	0	8.5	8.8	0
5	0	0.5	8.0	0	0.74
5	0	3	8.6	0	4.6
5	5	0.5	7.7	8.9	0.76

0163-1829/94/49(2)/881(7)/$06.00

III. DOWN-CONVERSION PROCESSES IN THE Yb-Tm, Yb-Ho, Tm-Ho, AND Yb-Tm-Ho SYSTEMS

In the GGG:Yb^{3+} sample the time evolution of the $^2F_{5/2}$ (Yb) level is exponential after a short-pulse excitation. The time constant is 1.47 ms. In the Yb-Tm or Yb-Ho codoped GGG samples the Yb fluorescence is strongly nonexponential and we explain this behavior by the Yb→Tm and Yb→Ho energy transfers (see Fig. 1).

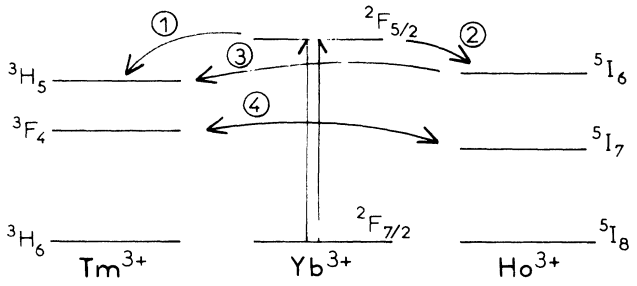

FIG. 1. Scheme of the Yb→Tm, Yb→Ho, and Tm↔Ho down-conversion energy transfers.

transfer(1)

$$^2F_{5/2}\ (\mathrm{Yb}),\ ^3H_6\ (\mathrm{Tm}) \rightarrow {}^2F_{7/2}\ (\mathrm{Yb}),\ ^3H_5\ (\mathrm{Tm}) ,$$

transfer(2)

$$^2F_{5/2}\ (\mathrm{Yb}),\ ^5I_8\ (\mathrm{Ho}) \rightarrow {}^2F_{7/2}\ (\mathrm{Yb}),\ ^5I_6\ (\mathrm{Ho}) .$$

These transfers are nonresonant: The gap between the Yb emission peak and the absorption peak is 900 cm^{-1} and 1400 cm^{-2} for Ho and Tm, respectively. The time evolution of the Yb fluorescence has been fitted with the Yokota-Tanimoto expression,[15] for example in the Yb-Ho case (and a similar expression in the Yb-Tm case):

$$N_D(t)=\exp\left[-\gamma t - bt^{1/2}\left[\frac{1+10.87+15.50x^2}{1+8.743x}\right]^{3/4}\right] \quad (1)$$

with

$$b=(4/3)\pi^{3/2}C_{\mathrm{Ho}}R_{DA}^3\gamma^{1/2} ,$$

$$x=D(\mathrm{Yb\text{-}Yb})R_{DA}^{-2}\gamma^{-1/3}t^{2/3},\quad D(\mathrm{Yb\text{-}Yb})=kC_{\mathrm{Yb}}^{4/3} ,$$

where $1/\gamma=1.47$ ms, C_{Ho} and C_{Yb} are the Ho and Yb concentrations, D(Yb-Yb) is the Yb diffusion constant, and R_{DA} is the critical radius of the Yb-Ho dipole-dipole interaction. The results of the fits are

transfer(1): $R_{DA}=1.06$ nm, $k=3\times10^7$ nm s^{-1}(5% Yb-5% Tm sample)

quantum yield=96% ,

transfer(2): $R_{DA}=1.3$ nm, $k=7.6\times10^7$ nm s^{-1}(5% Yb-0.5% Ho sample)

quantum yield=83% ,

$R_{DA}=1.14$ nm, $k=5.6\times10^7$ nm s^{-1}(5% Yb-3% Ho sample)

quantum yield=97% .

The experimental data and fits are shown in Fig. 2. The time evolution of the acceptor levels [$^3F_4$ (Tm) via the fast $^3H_5\rightarrow{}^3F_4$ deexcitation or $^5I_6$ (Ho)] have been obtained with the following expression:

$$N_A(t)=\int_0^t e(t-t')K_A(t')dt' , \quad (2)$$

where $e(t)=-(\dot{N}_D+\gamma N_D)$ is the transfer rate at time t [N_D is the donor population given by expression (1)], $K_A(t)=\exp(-t/\tau_A)$ is the response of the acceptor level to a δ excitation ($\tau_A=550$ μs for $^5I_6$ Ho level and 9 ms for $^3F_4$ Tm level).

In the doubly Yb-Ho-doped sample the $^5I_6$ level is a weak source of loss (1.7%) because its radiative deexcitation towards the $^5I_8$ level is weak: 29.4 s^{-1},[16] the whole deexcitation ($^5I_7+{}^5I_8$) being $1/(550\mu s)=1818^1$ s.

In the Yb-Tm-Ho tridoped sample the transfers (1) and (2) coexist but transfer (2) is now much weaker because of the high Tm concentration. Its quantum yield is estimated from decay time analysis to be about 1.5%, and that of transfer (1) remains 96%. Transfer (2) is now followed by transfer (3),

transfer(3): $^5I_6$ (Ho), $^3H_6$ (Tm)→$^5I_8$ (Ho), $^3H_5$ (Tm).

Transfer (3) is clearly seen by comparison of the $^5I_6$ (Ho) decay time in the Yb-0.5% Ho bidoped sample and in the Yb-Tm-0.5 Ho tridoped one, after a short excitation in the $^5T_5$ (Ho) level. It is much shorter in the tridoped case (see Fig. 3), corresponding to a 90% transfer quantum yield. Transfer (3) is explained by the good overlap between the $^5I_6$ emission and the $^3H_5$ absorption near 1200 nm.

In the triply doped sample the $^3H_5$(Tm) level is a negligible source of losses because its radiative deexcitation towards the $^3H_6$ is rather weak: 162 s^{-1} by comparison with its nonradiative deexcitation towards the $^3F_4$ level; 10^6 s^{-1}. More precisely we have established the energy gap law[17] in GGG relating the nonradiative multiphonon deexcitation rate W_{nf} of a Tm or Ho level in function of its energy gap ΔE with its next lower one:

$$W_{\mathrm{nr}}=W_{\mathrm{nr}}(0)e^{-\alpha\Delta E} . \quad (3)$$

The total probability of transition $1/\tau$ of a given level being such that

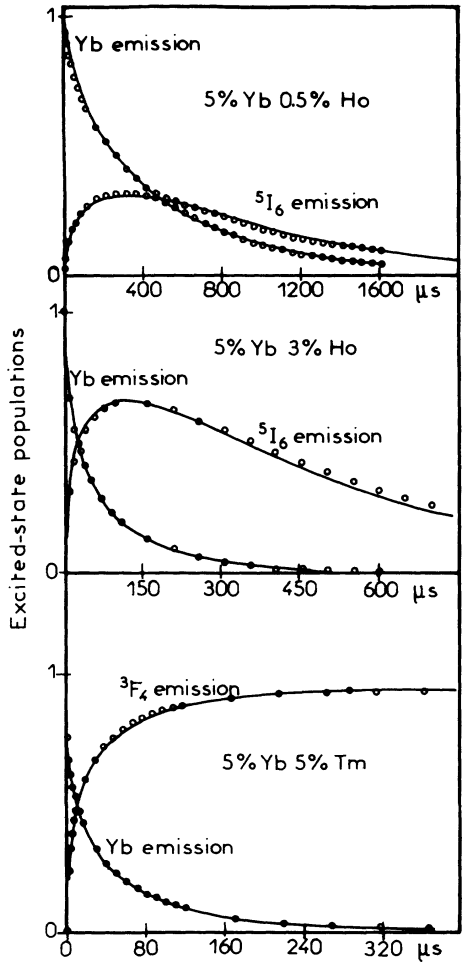

FIG. 2. Time evolutions of the Yb fluorescence and of the $^3F_4$ (Tm) or $^5I_6$ (Ho) fluorescences after a short excitation in Yb. The circles are the results of fits.

$$W_{nr}=1/\tau-W_{rad} \ . \tag{4}$$

In (4), W_{rad} was extracted from Ref. 16 for the Ho levels and from a Judd-Ofelt analysis[18] of the forced electric-dipole transition based on our own absorption measurements for the Tm levels (from $^3F_4$ to $^1D_2$, see their energy positions in Fig. 7). In this latter case we used the reduced matrix elements of the unit tensors $U^{(\lambda)}$ ($\lambda=2,4,6$) given in Ref. 19. The Judd-Ofelt parameters were found to be

$$\Omega_2=1.85\times10^{-21}\ \text{cm}^{-2} ,$$

$$\Omega_4=9.61\times10^{-21}\ \text{cm}^{-2} ,$$

$$\Omega_6=7.36\times10^{-21}\ \text{cm}^{2} ,$$

leading to a root-mean-square deviation of the measured and calculated line strengths of 9% of the average line strength.

The spontaneous deexcitation lifetime τ in (4) for a given Ho or Tm level was obtained by fitting its time evolution after a direct pulsed excitation (when it is not exponential) with the standard expression (1) in which we put $D=0$ for simplification.

The fitting of W_{nr} in (4) with expression (3), represented in Fig. 4, gives the following values:

$$W(0)=2.4\times10^{9}\ \text{s}^{-1} ,$$

$$\alpha=3.79\times10^{-3}\ \text{cm} .$$

We can say that the pumped energy in the Yb ions is returned with about 97% quantum yield on the $^3F_4$ (Tm) level in the triply Yb-Tm-Ho-doped sample and on the $^5I_7$ (Ho) level with a quantum yield of 83% $\times(1-.017)=81.6\%$ in the doubly Yb-Ho(0.5%) sample.

We have now to remember that the $^3F_4$(Tm) and$^5I_7$ (Ho) levels in the triply Yb-Tm-Ho-doped sample are coupled by transfer and back transfer (4),

transfer(4): $^3F_4$ (Tm), $^5I_8$ (Ho)$\leftrightarrow$$^3H_6$ (Tm), $^5I_7$ (Ho)

Their study was the motivation for our previous work[6] from which we can estimate that the maximum of the $^5I_7$ (Ho) population, reached 400 μs after the exciting pulse into the Yb ions, is about 55% of the feeding of the $^3F_4$ level, that is to say $0.55\times0.97=53.3\%$. We have to notice that the missing fraction ($0.45\times0.97=43.6\%$) is not lost but is stored into the $^3F_4$ (Tm) level because of the Ho→Tm back transfer and because this level is a metastable one. If depopulation of the $^5I_7$ (Ho) level is achieved by stimulated emission, the energy stored in the

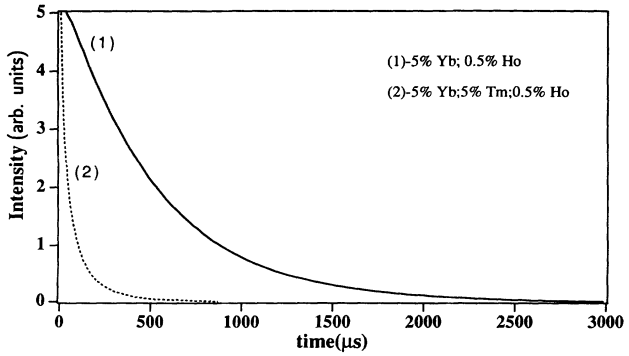

FIG. 3. Time evolution of the $^5I_6$ (Ho) fluorescence in the bidopoed Yb-0.5% Ho sample (curve 1) and in the tridoped Yb-Tm-0.5% Ho sample (curve 2), after a pulsed excitation in the $^5F_5$ (Ho) level.

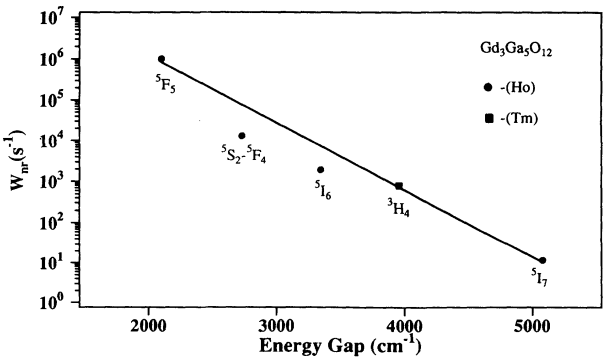

FIG. 4. Energy gap law in GGG relating the nonradiative multiphonon deexcitation rate of a level and its energy gap with its next lower level.

$^3F_4$ (Tm) level will be transferred to the $^5I_7$ (Ho) level and then can be used in its turn.

IV. UP-CONVERSION ENERGY LOSSES

A. Up-conversion quantum yields and power dependence

The excitation of the Yb ions is also followed by anti-Stokes emissions coming from upper Tm and Ho levels: 820 nm [$^3H_4$ (Tm)], 481 nm [$^1G_4$ (Tm)], 548 nm [$^5S_2$-$^5F_4$ (Ho)], 665 nm [$^5F_5$ (Ho)]. We have neglected them in the excited-state dynamics described in the previous section because they are rather weak: The quantum yields of these up-conversion processes are a few % in our conditions of excitations.

The up-conversion quantum yield from Yb ions towards a given Ho or Tm level has been obtained as the ratio of two intensities of fluorescence of this level following upon two excitations: one into the Yb ions and the other directly in the level (or in the level immediately above the given level, the energy gap between these two levels being weak enough to produce a fast nonradiative multiphonon deexcitation with 100% quantum yield; it is the case for the $^5F_3 \rightarrow {}^5S_2$-$^5F_4$ (Ho) deexcitation, see Fig. 4). The two intensities of fluorescence were integrated over time and related to the same number of absorbed photons (the incident and transmitted energies of the laser beam were measured at known wavelengths).

The results are gathered in Table II, except for the $^5S_2$-$^5F_4$ (Ho) level in the triply doped sample because in this case we used an excitation into the $^2F_5$ (Ho) level which could be slightly absorbed by the $^1G_4$ (Tm) level. Nevertheless we give in Fig. 5 the time evolution of the $^5S_2$-$^5F_4$ (Ho) fluorescence after excitation in the Yb ion, related to the same number of absorbed photons by the Yb ions. The three curves reflect the relative $^5S_2$-$^5F_4$ (Ho) populations in the three Ho-doped samples and we can see that the one in the triply doped sample remains much weaker than the ones in the doubly doped samples, the latter being feeded with a weak quantum yield: 4.4% maximum.

The above measurements have been done by exciting Yb ions with a laser beam of energy from 1.6 up to 2 mJ/pulse but we have also measured the power dependence of the up-conversion and $^5I_6$ (Ho) intensities of fluorescence at the top of their time evolution. We also measured the power dependence of the Yb emission. The results for two measurements are shown in Fig. 6. The data were fitted with a E^n law. n is given in Table III for the different emissions. We expect that n should be an in-

TABLE II. Up-conversion quantum yields after infrared excitation into Yb ions.

Crystal	Level	Quantum yield %
5% Yb 0.5% Ho	$^5S_2$-$^5F_4$	2.7
5% Yb 3% Ho	$^5S_2$-$^5F_4$	4.4
5% Yb 5% Tm	$^3H_4$	6.0
5% Yb 5% Tm	$^1G_4$	0.03
5% Yb 5% Tm 0.5% Ho	$^3H_4$	5.1

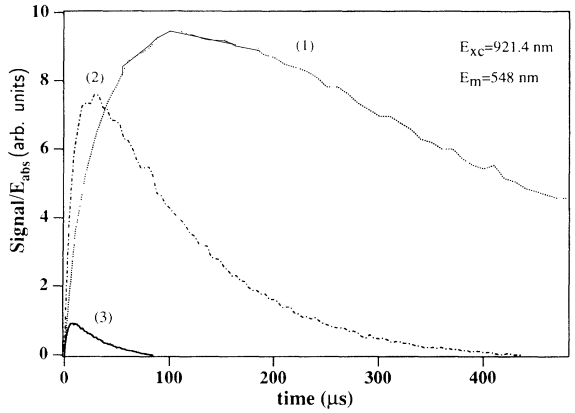

FIG. 5. Relative populations in the three Ho-doped samples of the $^5S_2$-$^5F_4$ (Ho) level after excitation into Yb ions. Curves (1) 5% Yb–0.5% Ho, (2) 5% Yb–3% Ho, (3) 5% Yb–0.5% Ho–5% Tm.

TABLE III. Power dependence of the intensities of fluorescence after excitation in Yb ions.

Emission	n
$^2F_{5/2}$ (Yb)	1
$^5I_6$ (Ho)	1
$^5F_5$ (Ho)	2
$^5S_2$-$^5F_4$ (Ho)	2.5
$^3H_4$ (Tm)	1.7
$^1G_4$ (Tm)	2.55

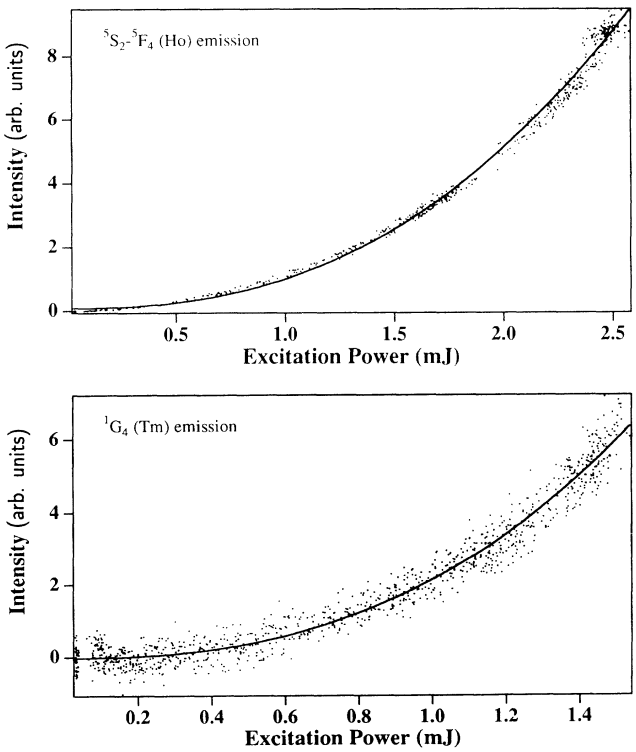

FIG. 6. Power dependence of the intensities of fluorescence at the top of their time evolution after excitation in Yb ions. Each point is an experimental result, the solid curves are results of fits.

teger (1,2,3) depending if the process is a one-, two-, or three-photon process. Noninteger values of the exponent could be explained by partial saturation of one transfer step or by the fact that the excitation of the level involves a mixing of processes with different numbers of photons.

B. Up-conversion excited-state dynamics

Let us consider first the Yb-Ho or Yb-Tm bidoped samples. After excitation of Yb ions the only levels which are strongly and simultaneously populated are the $^2F_{5/2}$ (Yb)-$^5I_6$-$^5I_7$ (Ho) or $^2F_{5/2}$ (Yb)-$^3F_4$ (Tm) due to transfers (2) and (1) (Fig. 1). Then the simplest hypothesis is to explain the up-conversion recorded fluorescences by transfers (5), (6), (7), (8) (see Fig. 7).

Transfers (5) and (6) are probable due to the overlap between the Yb emission cross section and the $^5I_6 \rightarrow {}^5S_2$-$^5F_4$ (Ho) and the $^5I_7 \rightarrow {}^5F_5$ (Ho) excited-state absorption cross sections (Fig. 8). These cross sections were deduced from McCumber relations connecting emission and absorption spectra.[20] The Yb emission cross section $\sigma_e(\omega)$ is related to the Yb emission spectrum $f(\omega)$ at frequency ω:

$$f(\omega)=\sigma_e(\omega)(\omega n/2\pi c)^2 \tag{5}$$

and $f(\omega)$ is normalized such that

$$1/\tau=8\pi\int f(\omega)d\omega/2\pi \ . \tag{6}$$

In (6) the Yb radiative lifetime (1.47 ms) was taken as the spontaneous lifetime deexcitation in the Yb single-doped sample.

The $^5I_6 \rightarrow {}^5S_2$-$^5F_4$ (Ho) and the $^5I_7 \rightarrow {}^5F_5$ (Ho) excited-state absorption cross sections $\sigma_a(\omega)$ are obtained knowing first the emission cross section $\sigma_e(\omega)$:

$$\sigma_a=\sigma_e\exp(\hbar\omega/kT)(N_2/N_1)_e \ . \tag{7}$$

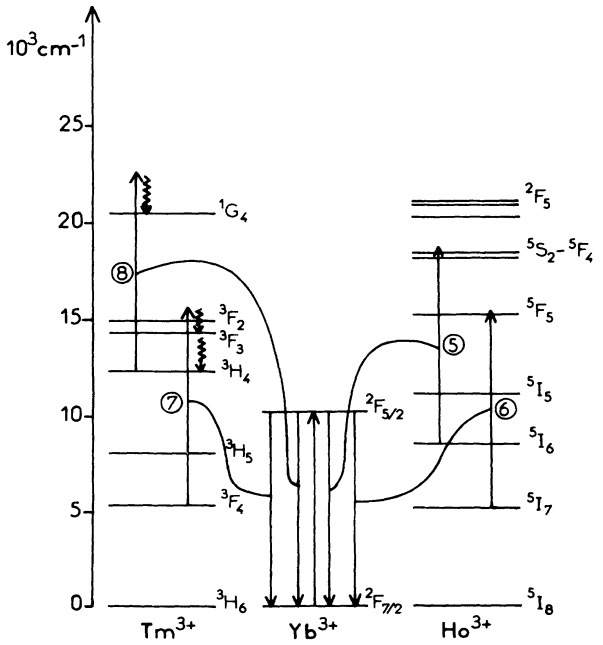

FIG. 7. Scheme of the up-conversion energy transfers.

In (7), σ_e was obtained with relations similar to (5) and (6) after recording the corresponding emission spectra, the radiative lifetime in (6) being taken from:[16] 3.85 and 1.89 ms for transfers (5) and (6), respectively. $(N_2/N_1)_e$ is the ratio at thermal equilibrium of the two excited-state populations involved in the transition. It is calculated by Boltzman law and requires the positions of the Stark sublevels. The Ho ions substitute the Gd ones and are in D_2 symmetry sites. In this case each $^{2S+1}L_J$ manifold of Ho^{3+} is split into $2J+1$ sublevels, labeled $\Gamma_1,\Gamma_2,\Gamma_3,\Gamma_4$ corresponding to the irreducible representations of the D_2 point group. Because neither electric nor magnetic dipole transitions are allowed between sublevels corresponding to the same irreducible representation[21] the positions of some of them cannot be found without crystal-field calculation even with low-temperature absorption and emission measurements. So Boltzman law was applied using only the range of energy in which the Stark sublevels of a given manifold are distributed, the distribution being taken as a continuous one. Then assuming a dipole-dipole interaction between Yb and Ho ions, we have calculated the critical radius R of the up-conversion energy transfer with the Dexter formula:[22]

$$R^6=\tau(1/2\pi)^4(6c/n^2)\int\sigma_e(\lambda)\sigma_a(\lambda)d\lambda \ , \tag{8}$$

where τ is the Yb radiative lifetime, σ_e is the Yb emission cross section, and σ_a is the $^5I_6 \rightarrow {}^5S_2$-$^5F_4$ (Ho) or the

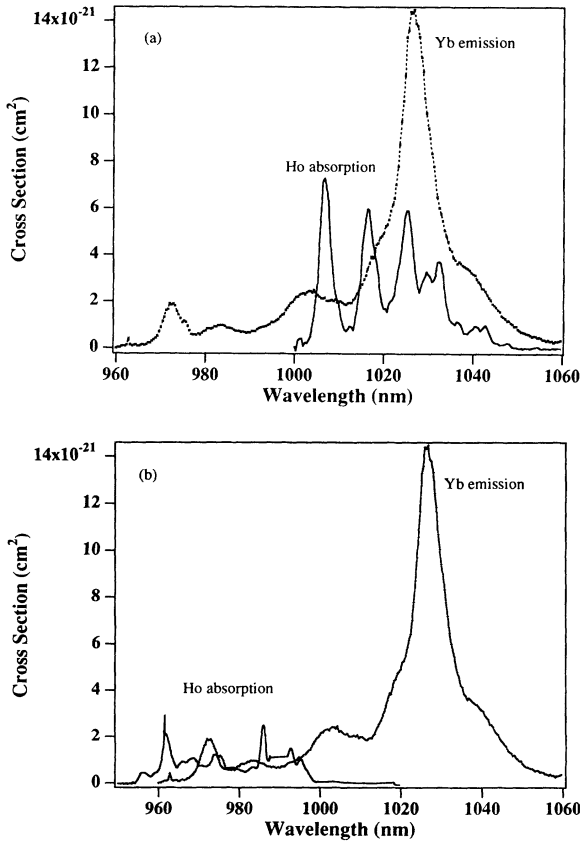

FIG. 8. Spectral overlap between the Yb emission cross section: (a) the $^5I_6 \rightarrow {}^5S_2$-$^5F_4$ (Ho) and (b) the $^5I_7 \rightarrow {}^5F_5$ (Ho) excited-state absorption cross sections.

$^5I_7 \rightarrow {}^5F_5$ (Ho) excited-state absorption cross section. The result is $R = 1.19$ and $R = 0.77$ nm for transfers (5) and (6), respectively.

Transfers (7) and (8) are not resonant. Their energy gaps are respectively, 660 and 770 cm^{-1} but the examples of nonresonant transfers (1) and (2) show that even in this case they can be efficient in GGG.

We turn now to a tentative model of the time evolution of the $^5S_2$-$^5F_4$ (Ho) and $^3H_4$ (Tm) fluorescence after excitation of the Yb ions, in the bidoped Yb-Ho and Yb-Tm samples. In other words we want to model the dynamics of up-conversion energy transfers (5) and (7). The time evolution $N_A(t)$ of the population of an acceptor level A such as $^5S_2$-$^5F_4$ (Ho) and $^3H_4$ (Tm) levels is given by expression (2), in which we have chosen as $K_A(t)$ an Inokuti-Hirayama expression[23] because after a direct pulsed excitation their populations do not decay exponentially: They are subjected to efficient down-conversion energy transfers. In Fig. 9, these nonexponential time dependences are represented by curves (1) (solid lines) and the $K_A(t)$ functions [given by expression (1) in which the diffusion constant D is zero] are represented by circles (1) after an adequate choice of the γ and b parameters in expression (1).

We have now to choose the source $e(t)$ in expression (2). A first attempt consisted in taking the product of the two time evolutions of Yb and $^5I_6$ (Ho) emissions for transfer (5) and of Yb and $^3F_4$ (Tm) for transfer (7). The populations were obtained in Sec. III when transfers (1) and (2) were studied. Their products are shown by curves (3) in Fig. 9. We see that our model is not able to reproduce the experimental data represented by solid curves (2), *in particular the fast observed rise time.* We could put forward the saturation of transfers (1) and (2) or partially add to transfer (5) a three-photon process. Of course in a complete model these phenomena should be taken into account (we said that they were convenient to explain noninteger exponents in the power dependence of the fluorescence) but we believe that they can only *prolong* the rise time and not shorten it. If our model fails to describe the rapidity of the dynamics of the up-conversion process it is due to the fact that it supposes the same yield of up-conversion transfer for all the Yb-Ho or Yb-Tm ions pairs whatever the interatomic distance. In fact, because of the fluctuations of ion distribution, in the regions of the crystal where the donor/acceptor ions are closer, the coefficients of transfer are larger and a more important contribution to the up-conversion process is expected. This important phenomenon is often considered for down-conversion energy transfers but rarely for up-conversion processes for which equations of population are extensively used. The following model taking it into account has been tested.

We decompose[24,25] the population $N_D(t)$ of the $^2F_{5/2}$ (Yb) level in function of the transfer yield ϕ on the $^5I_6$ (Ho) or $^3H_5$ (Tm) acceptor level [transfers (2) or (1)]:

$$N_D(t) = \int N_{D\phi}(t)\,d\phi \quad \text{with } N_{D\phi} = w(\phi)e^{-t(\gamma+\phi)} , \tag{9}$$

where

$$w(\phi) = \phi^{-3/2} e^{-b^2/4\phi} . \tag{10}$$

In (9) and (10), γ and b are given in expression (1). The acceptor population [$^5I_6$ (Ho) or $^3H_5$ (Tm) levels] created by the Yb excited ions belonging to class ϕ is labeled $N_{D'\phi}(t)$. A general expression for the excitation $e(t)$ in expression (2) is a sum over all the products $N_{D\phi}(t)N_{D'\phi}(t)$:

$$e(t) = \int\int a(\phi,\phi')N_{D\phi}(t)N_{D'\phi'}(t)\,d\phi\,d\phi' , \tag{11}$$

where $a(\phi,\phi')$ is an unknown function whose value was 1

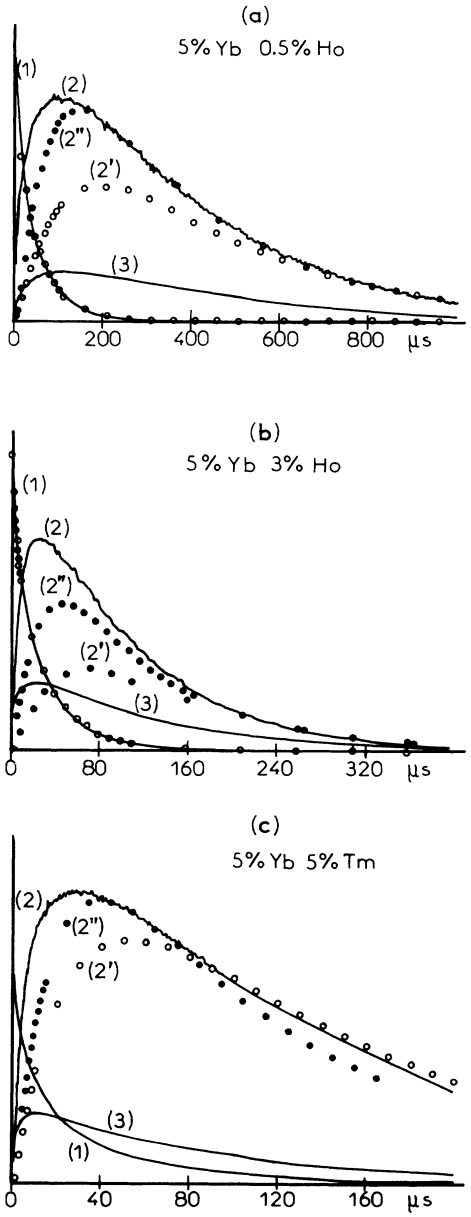

FIG. 9. Time evolution of the (a) and (b) $^5S_2$-$^5F_4 \rightarrow {}^5I_8$ (Ho) fluorescence, (c) $^3H_4 \rightarrow {}^3H_6$ (Tm) fluorescence. Curve (1) (experimental) and circles (1) (theoretical) are fluorescences obtained after a direct δ excitation, Curve (2) (experimental) and circles (2′) and (2″) (theoretical) are fluorescences obtained after a δ excitation into the Yb ions, and Curve (3) are the theoretical time evolutions of the source $e(t)$ used in expression (2) to obtain circles (2′).

in the previous model and representing the up-conversion probability. In order to obtain a faster rise time from expression (2) we have to give a larger weight in expression (11) to the products $N_{D\phi}(t)N_{D'\phi}(t)$ having a large ϕ. That means that the excited Yb ions which are close to acceptor ions in a part of the crystal will have simultaneously a large yield ϕ of transfer (1) or (2) and a large probability of up-conversion $a(\phi,\phi')$. Taking $a(\phi,\phi')=\phi$ in expression (11) inserted in expression (2), we obtain the circles (2'') in Fig. 9. The experimental rise times are now much better. So despite the fact that our model is not rigorous it proves that a good description of up-conversion dynamics must take into account the fluctuations of distribution of relative positions of the donor/acceptor ions.

V. CONCLUSION

We have shown that efficient down-conversion energy transfers drive the pump energy into Yb ions towards the $^5I_7$ 2-μm emitting laser level of the Ho^{3+} ions. We have measured the quantum yield of the up-conversion energy losses in the Yb-Ho and Yb-Tm bidoped samples. They are not more than 4.4% in our condition of excitation. In the triply Yb-Tm-Ho-doped sample the up-conversion energy losses in Ho^{3+} ions are even weaker (Fig. 5) because they are quenched by the resonant $^5I_6$ (Ho)$\rightarrow{}^3H_5$ (Tm) transfer. Moreover, efficient cross-relaxation mechanisms down convert the up-converted energy from the upper Ho and Tm energy levels to the ground state, since the fluorescence time dependence of the former is not exponential when they are directly excited. The counterpart of the addition of Tm ions in the material is the storage of a fraction of the energy into the $^3F_4$ (Tm) level.

We have shown that both up-conversion and down-conversion dynamics cannot be described correctly if the fluctuations of distribution of the donor and acceptor positions are not taken into account.

ACKNOWLEDGMENTS

This work was supported by the Defense Ministry (France) (DGA/DRET) under Grant No. 90/130, by Région Rhône-Alpes and CNRS. The CNPq of Brazil is thanked for supporting L. C. Courrol. The Laboratoire de Physico-Chimie des Matériaux Luminescents is Unité de Recherche Associée au CNRS No. 442.

[1]A. Erbil and H. P. Jenssen, Appl. Opt. **19**, 1729 (1980).
[2]E. W. Duczynski, G. Huber, V. G. Ostroumov, and I. A. Shcherbakov, Appl. Phys. Lett. **48**, 1562 (1986).
[3]T. Y. Fan, G. Huber, R. L. Byer, and P. Mitzscherlich, IEEE J. Quant. Electron. **QE-24**, 924 (1988).
[4]S. R. Bowman, M. J. Winings, S. Searles, and B. J. Feldman, IEEE J. Quant. Electron. **QE-27**, 1129 (1991).
[5]A. Brenier, C. Madej, C. Pédrini, and G. Boulon, J. Phys.: Condens. Matter **3**, 203 (1991); **3**, 7887 (1991).
[6]A. Brenier, G. Boulon, C. Madej, C. Pédrini, and L. Lou, J. Lumin. **54**, 271 (1993).
[7]G. Armagan, A. M. Buoncristiani, C. H. Bair, A. T. Inge, and R. V. Hess, *OSA Proceedings on Advanced Solid State Lasers, 1991*, edited by George Dubb and Lloy Chase (Optical Society of America, Washington, DC, 1991), Vol. 10.
[8]R. R. Petrin, M. G. Jani, R. C. Powell, and M. Kokta, Opt. Mater. **1**, 111 (1992).
[9]J. L. Sommerdijk, W. L. Wanmaker, and J. G. Verriet, J. Lumin. **4**, 404 (1971).
[10]J. L. Sommerdijk, J. Lumin. **4**, 441 (1971).
[11]B. M. Antipenko, S. P. Voronin, Sh. N. Gifeisman, R. V. Dubravyanu, Yu. E. Perlin, T. A. Privalova, and O. B. Raba, Opt. Spektrosk. **58**, 1270 (1985) [Opt. Spectrosc. (USSR) **58**, 780 (1985)].
[12]F. W. Ostermayer, Jr., J. P. Van der Ziel, H. M. Marcos, L. G. Van Uiter, and J. E. Geusic, Phys. Rev. B **3**, 2698 (1971).
[13]M. A. Chamarro and R. Cases, J. Lumin. **42**, 267 (1988).
[14]R. K. Watts and H. J. Richter, Phys. Rev. B **6**, 1584 (1972).
[15]M. Yokota and O. Taminoto, J. Phys. Soc. Jpn. **22**, 779 (1967).
[16]Q. Wang, S. Zhang, S. Wu, and X. Dong, J. Lumin. **40&41**, 181 (1988).
[17]M. J. Weber, Phys. Rev. B **8**, 54 (1973).
[18]B. R. Judd, Phys. Rev. **127**, 750 (1962).
[19]N. Spector, R. Reisfeld, and L. Boehm, Chem. Phys. Lett. **49**, 49 (1977).
[20]D. E. McCumber, Phys. Rev. **136**, 954 (1964).
[21]J. B. Gruber, M. E. Hills, M. Seltzer, S. B. Stevens, C. A. Morrison, G. A. Turner, and M. R. Kokta, J. Appl. Phys. **69**, 8183 (1991).
[22]D. L. Dexter, J. Chem. Phys. **21**, 836 (1953).
[23]M. Inokuti and F. Hirayama, J. Chem. Phys. **43**, 1978 (1965).
[24]A. Brenier, Thèse de Doctorat, University Claude Bernard-Lyon I, 1991.
[25]A. Brenier, C. Madej, C. Pédrini, and G. Boulon, J. Phys.: Condens. Matter **3**, 203 (1991).